HHS Public Access

Author manuscript

J Med Chem. Author manuscript; available in PMC 2017 July 14.

Published in final edited form as:

J Med Chem. 2016 July 14; 59(13): 6012–6024. doi:10.1021/acs.jmedchem.5b01975.

Lanthanides: Applications in Cancer Diagnosis and Therapy

Ruijie D. Teo[†], **John Termini**[*,‡], and **Harry B. Gray**[*,†]

[†] Division of Chemistry and Chemical Engineering, California Institute of Technology, Pasadena, California 91125, USA

[‡] Department of Molecular Medicine, Beckman Research Institute of the City of Hope, 1500 E. Duarte Road, Duarte, California 91010, USA

Abstract

Lanthanide complexes are of increasing importance in cancer diagnosis and therapy, owing to the versatile chemical and magnetic properties of the lanthanide-ion 4f electronic configuration. Following the first implementation of gadolinium(III)-based contrast agents in magnetic resonance imaging in the 1980s, lanthanide-based small molecules and nanomaterials have been investigated as cytotoxic agents and inhibitors, in photodynamic therapy, radiation therapy, drug/gene delivery, biosensing, and bioimaging. As the potential utility of lanthanides in these areas continues to increase, this timely perspective of current applications will be useful to medicinal chemists and other investigators interested in the latest developments and trends in this emerging field.

Graphical Abstract

[*]**Corresponding Authors** John Termini: jtermini@coh.org; Harry B. Gray: hbgray@caltech.edu.

The authors declare no competing financial interest.

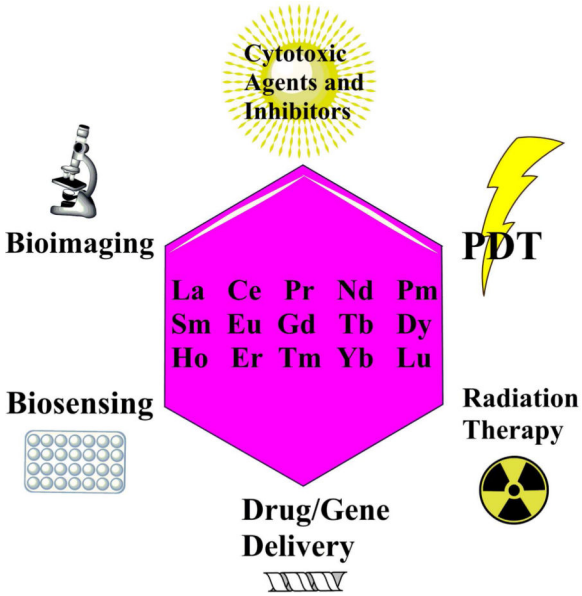

1. Introduction

The problem of cancer is not new. It was recently reported that the oldest evidence of this disease was found in the remains of a 4,200 year old Egyptian woman.[1] As cancer existed long before written history, it is no surprise that many different means of medical treatment have arisen. Some early treatments included the cauterization of tumors, and the ingestion of boiled barley mixed with nuts to treat stomach cancer.[2] In 2015, the American Cancer Society estimated that about 1,600 people in the United States will die of cancer every day.[3] Owing to this epidemic threat, modern-day cancer diagnostic and therapeutic approaches have been evolving rapidly. In particular, a very powerful diagnostic method involves magnetic resonance imaging (MRI) in which metal-based contrast agents are administered to improve image resolution.

Chemotherapy, radiation therapy (XRT), and targeted therapy are some of the main types of cancer therapy. Chemotherapy involves drugs to kill cancer cells, while XRT uses high doses of radiation to eliminate tumors. Targeted therapy, as the name suggests, often uses small-molecule drugs or monoclonal antibodies to target specific proteins that drive cancer cell proliferation. Small-molecule based drugs include inorganic compounds – most importantly the widely used cis-dichlorodiammineplatinum(II), better known as cisplatin. Indeed, metals are used extensively in cancer diagnosis and therapy, and the lanthanides occupy an important niche in these areas.

Lanthanides are elements with atomic numbers ranging from 57 (lanthanum) to 71 (lutetium). They also are known as “rare earth” elements, because they were once thought to be present in very small amounts in the Earth's crust. However, we know today that lanthanides are relatively abundant. In 1803, the first lanthanide, cerium, was discovered in its mineral form – cerite.[4] As lanthanides are extremely unstable when isolated in elemental form, they often are found as oxides and fluorides in rocks, ores, and minerals. As methods

for the extraction and separation of these lanthanides salts continue to improve, many investigators have turned their attention toward utilizing these elements in cancer imaging and therapy. The redox stability of Ln^{3+} ions makes them highly suitable for cellular applications in the presence of biological reducing agents like ascorbate and thiols, with the added advantage of favorable luminescent properties attributable to 4f↔5d, charge-transfer, and f↔f transitions.[5] Currently, gadolinium-containing complexes – gadopentetic acid (Magnevist®) and gadoteric acid (Artirem®) – are commonly used as MRI contrast agents for cancer imaging,[6] while lanthanide radioisotopes like ^{177}Lu have been used in cancer imaging and therapy.[7] Other forms of lanthanides, such as lanthanide oxide nanoparticles, nanodrums, and nanocrystals are promising as imaging agents and potential anticancer drugs.[8] For example, CeO_2 nanoparticles (Nanoceria) are used to inhibit the deleterious effects of reactive oxygen intermediates and are under development as potential therapeutic agents.[9] However, the biomedical applications of lanthanides extend well beyond their use as routine cancer therapeutics and imaging agents, and publications detailing their use have increased over the last 10 years (Figure 1). Our Perspective highlights current work as well as insights that could drive future applications for this class of metals in cancer diagnosis and therapy – more specifically, we discuss recent developments in cytotoxic lanthanide agents and inhibitors, photodynamic therapy (PDT), XRT, drug/gene delivery, biosensing, and bioimaging. In addition, elements such as yttrium whose properties are similar to those of the lanthanides will be included throughout.

2. Cytotoxic Agents and Inhibitors

One of the earliest applications of lanthanides in cancer therapy was reported by Anghileri and coworkers,[10] who emphasized the importance of cationic cell membrane interactions in mediating Ln cytotoxicity. Following this work, other lanthanide-based anticancer agents were reported, with ones featuring complexation with a wide range of ligands, including hymecromone, umbelliferone, mendiaxon, warfarin, coumachlor and niffcoumar, coumarin-3-carboxylic acid, and dihalo-8-quinolinoline (Scheme 1: 2-Gd, 2-Sm, 2-Eu, 2-Tb, 2-Dy, 3-Dy, 3-Er).[11,12,13,14] Recently it was shown that oxoglaucine-lanthanide complexes (1-Y and 1-Dy) exhibited significantly greater cytotoxicity than the corresponding $Ln(NO_3)_3$ salts.[15] It was found that 2-Gd and 3-Dy interacted more strongly with DNA than the quinolinol ligand, with intercalation the most probable binding mode;[12] and 1-Dy triggered DNA damage in hepatocellular carcinoma HepG2 cells, resulting in S phase cell cycle arrest and apoptosis.[15] Most notably, 3-Dy (IC_{50}: 18.3 ± 1.0 nm) and 3-Er (IC_{50}: 31.5 ± 1.2 nm) are highly cytotoxic towards BEL-7404 human hepatocellular carcinoma cells, while both cisplatin (IC_{50}: 132.8 ± 1.2 μM) and corresponding salts $Dy(NO_3)_3$ and $Er(NO_3)_3$ showed little to no cytotoxicity.[12] Although the cytotoxic action of lanthanide complexes is typically attributed to their interactions with DNA, other mechanisms have been proposed: Pr^{3+}, La^{3+}, and Nd^{3+} were found to inhibit calcium transport in mitochondria (owing to similar ionic radii),[16] and Yb-OEP-treated cells (Scheme 1) were found to undergo endoplasmic reticulum stress pathway-mediated apoptosis, with IC_{50} values in the sub-micromolar range.[17] Other notable mechanisms include the inhibition of thioredoxin reductase[18] and targeting of the glutathione-independent lipoate reduction pathway by gadolinium(III)

texaphryin (MGd, Xcytrin®) (Scheme 1),[19] subsequently inhibiting cancer cell DNA replication, repair, and inducing oxidative stress.

In addition to small molecules, lanthanide nanomaterials (such as Nanoceria) are cytotoxic to several types of human cancer cells *in vitro*, including squamous cell carcinoma, hepatocellular carcinoma, alveolar epithelial cancer cells, and pancreatic carcinoma.[20] These toxicities can be attributed to the induction of oxidative stress, the activation of mitogen-activated protein-kinase (MAPK) signaling pathways, and the mimicking of superoxide dismutase, glutathione peroxidase, and catalase activities.[20-21]

A limitation associated with employment of the aforementioned lanthanide complexes and nanoparticles is selectivity – targeting cancer cells while leaving noncancerous cells unaffected. In order to overcome this problem, lanthanides are often conjugated to proteins or nucleic acids in order to confer specificity for more precise inhibition of proteins, and increased utility for imaging applications. Lanthanide-doped upconversion nanoparticles (UCNPs) can be conjugated to polo-like kinase 1 (Plk1)-specific peptides, enabling real-time imaging (980 nm excitation) while protecting these peptides from enzymatic degradation and inhibiting Plk1.[22] Among the different $NaGdF_4@SiO_2$-P_n systems (spherical and cubic) investigated, spherical $NaGdF_4@SiO_2$-P_n inhibited HeLa cells selectively (IC_{50}: 31.6 μg/ml) by causing G2 phase arrest while remaining nontoxic to normal cells.[22] Other similar cell-permeable systems include surface functionalized lanthanide nanoparticles UCNP-P_1 (Scheme 1) with cyclin D-specific peptides that inhibit the cyclin-dependent kinase 4 (CDK4)/cyclin D complex,[23] a promising anticancer target. As monoclonal antibody-drug conjugates such as trastuzumab emtansine and brentuximab vedotin have gained FDA approval,[24] we expect that research in lanthanide antibody conjugates for therapeutic applications will experience rapid growth.

3. Photodynamic Therapy

a. UV-vis Photodynamic Therapy

Ultraviolet-visible (UV-vis) PDT is a promising modality for cancer treatment, owing to its precise tumor targeting ability. Upon UV-vis irradiation, a photosensitizer is initially excited to a singlet state that can undergo intersystem crossing (ISC) to a triplet state. The newly formed triplet state of the photosensitizer can react with molecular oxygen to generate singlet oxygen ($^1O_2$), a very powerful oxidant, which destroys malignant cells within its diffusion path. A singlet-oxygen generator, Photofrin®, a porphyrin-based drug that absorbs strongly in the Soret region, has been approved by the FDA for endobronchial and esophageal cancers. Lanthanide-based compounds also are very suitable for PDT as ISC is facilitated, owing to the heavy atom effect,[25] which in turn promotes the generation of singlet oxygen. As a result, many lanthanide- substituted porphyrins and porphyrin analogs are potential PDT agents. The diamagnetic lutetium(III) texaphyrin (MLu, Lutrin®) (Scheme 1) localizes selectively in neoplastic tissues and generates singlet oxygen in 11% quantum yield in water.[26] By irradiating at 732 nm (150 J cm^{-2} at 150 mW cm^{-2}) at 3 h post-injection, 100% tumor ablation was observed in DBA/2N mice bearing fast-growing spontaneous mouse mammary tumor subline neoplasms of moderate size (70±35 mm^3) with a dosage of 10 μmol kg^{-1}. Other examples of lanthanide porphyrins include the water-

soluble, mitochondria-permeable erbium(III) complex Er-L (Figure 2), which induced photocytotoxicity towards HeLa cells *in vitro* with modest formation of singlet oxygen (Φ_Δ = 0.10),[27] and gadolinium complexes Gd-N and Gd-RhB (Figure 3a) that effectively inhibited HeLa-tumors in BALB/c nude mice.[28] Gd-N is an especially potent photosensitizer (51% singlet oxygen quantum yield) that specifically targets tumor cells via anionic phosphatidylserine membranes (Figures 3b-d), enabling the monitoring of laser-excited photoemission signals for live cancer cell tracking and imaging.

Lanthanide-doped nanoparticles are of intense interest, owing to long-lived luminescences, large antenna-generated Stokes or anti-Stokes shifts, narrow emission bands, high resistance to photobleaching, and low toxicity.[29] In particular, lanthanide-doped UCNPs are promising photosensitizers for near-infrared (NIR)-triggered PDT. Aptly named, these UCNPs convert NIR light to visible light and offer remarkable light penetration depth without interference from auto-fluorescence in biological specimens under excitation.[30] Recently, Wang and coworkers[31] showed a large reduction in cell viability for MDA-MB-231 cells incubated with UCNP–ZnPc-COOH for 24 h and irradiated with a 980 nm NIR laser at 0.5 W cm^{-2} for 10 min. *In vivo* PDT efficacy also was demonstrated in H22 tumor-bearing mice under similar NIR irradiation conditions 3 tumor volume in control mice increased from 248 to 1282 mm^3 after two weeks, whereas tumors in treated mice only increased from 240 to 501 mm^3 (Figures 4a,c) over the same period. Hematoxylin–eosin staining of tumor slices detected apoptotic and necrotic tumor cells, as shown in Figure 4d.

An unusual example of *in vivo* PDT illustrating the multi-functional modality of lanthanides was provided by treatment of U87MG tumor-bearing nude mice with chlorin e6 (Ce6)-loaded UCNPs (UCNP-Ce6) followed by 980 nm irradiation (Figure 5).[32] In addition to therapeutic tumor inhibition, these UCNPs also exhibited dual-modal imaging, as will be discussed below.

b. X-ray Induced Photodynamic Therapy

X-ray excited optical luminescence of lanthanide-based nanoparticles is an attractive alternative to conventional light sources in traditional PDT due to the potential for deep tissue penetration.[33] This unique therapy, first described by Chen and coworkers,[34] relies on activation of scintillation nanoparticles by x-rays to produce optical emission that activates photosensitizers, which in turn produce cytotoxic ROS. Subsequently, many lanthanide-based nanoparticles for x-ray induced PDT have been reported, including lanthanide-based micelles integrated with hypericin,[35] as well as a porphyrin-conjugated Tb_2O_3 nanoparticles.[36] Energy transfer between the nanoscintillator and the porphyrin was demonstrated under UV excitation for the porphyrin-nanoparticle conjugate, while the yield of $^1O_2$ increased with longer X-ray irradiation times.

4. Radiation Therapy

As poor penetration of UV-vis light often has rendered PDT unsuitable for treating deep-seated tumors, XRT (not to be confused with x-ray induced PDT) has gained popularity in recent years due to the potential for deep tissue targeting of tumors without the requirement for photosensitizers. After release from atoms irradiated with x-rays, inner shell electrons

react with water and oxygen, generating free radicals and causing tissue damage via secondary reactions.[37] Over the past few decades, many methods of using lanthanides in several types of XRT – brachytherapy, external beam radiotherapy, systemic radioisotope therapy with unsealed radiation sources – have been developed. In radioimmunotherapy, a ^{177}Lu–labeled anti-prostate-specific membrane antigen (PSMA) monoclonal antibody J591, induced a measurable response rate in metastatic castration-resistant prostate cancer in a Phase II clinical trial (Figure 6).[38]

One of the first lanthanide-based metal-ligand complexes considered for XRT was MGd, which kills malignant cells via endocytosis by a clathrin-dependent pathway and subsequent induction of apoptosis.[39] However, the efficacy of MGd as a general radiosensitizing agent is still debatable as it did not inhibit potentially lethal damage repair (repair of double-stranded breaks) in murine breast cancer EMT6 cells[40] and negative radiosensitivity results were obtained in two tumor models.[41] Yttrium, a rare-earth element that is congeneric with lanthanides, has been incorporated into ibritumomab tiuxetan (Zevalin) – an FDA-approved drug that has been effective in treating B-cell non-Hodgkin's lymphoma.[42] By attaching the murine anti-CD20 antibody ibritumomab to β^--emitting ^{90}Y via the linker-chelator tiuxeton, radiation can be selectively deposited in CD20+ cells.[43] This use of antibodies for targeted XRT is otherwise known as radioimmunotherapy (RIT).

More recently, lanthanide-based nanoparticles have been investigated as RIT agents. Typically, these radiosensitizing nanoparticles are composed of a core, a shell, and a surface. The core is made of elements like lanthanides for increased photon absorption. The shell acts as a base on which surface molecules are attached; and it also can confer additional properties such as the retention of radioactive daughter elements after decay. The surface molecules confer selectivity to the nanoparticles through the anchoring of site-, tissue-, cell- and/or receptor-specific molecules. One such example is a gold-coated lanthanide phosphate nanoparticle ($\{La_{0.5}Gd_{0.5}\}PO_4$@$GdPO_4$@Au) containing the therapeutic radionuclide ^{225}Ac that can act as an *in vivo* α-emitter, which is an advantage over β^- emitters due to their shorter range of emission (50–100 μm) along with high linear energy transfer.[44] Additionally, effective cell killing can be expected in hypoxic tumors since cytotoxicity is oxygen independent. These advantages could provide the impetus for further development of 'α-radioimmunotherapeutics'.

5. Drug/Gene Delivery

Owing to the very high charge to volume ratios of tripositive lanthanides, which facilitate the formation of Ln^{3+}-adenovirus complexes, several Ln cations were investigated for their ability to enhance transduction efficiency of adenovirus vectors *in vitro* and *in vivo*.[45] La^{3+} was found to be superior to Gd^{3+}, Y^{3+}, Lu^{3+}, and even Ca^{2+}. Lanthanide oxide nanostructures are promising drug delivery materials due to their ease of synthesis and exceptionally low dimensionality. Sm_2O_3 and Gd_2O_3 ultrathin nanosheets[46] were found to exhibit promising pH-controlled anticancer drug-delivery properties (Figure 7). Interestingly, fast 5-fluorouracil release was found at pH 4.0 relative to pH 7.4. The fast release behavior was attributed to the alkaline nature of nanosheets, which makes them highly attractive due to the acidic environment of tumor cells.

Several lanthanide-doped nanomaterials, in particular UCNPs, act as drug and gene delivery systems.[47] These UCNPs are popular since they can be used as image-guided therapy (IGT) agents – see discussions in later sections of this Perspective. However, there are still many possibilities to be explored in the field of drug/gene delivery. The incorporation of lanthanides in smart polymers that respond to chemical and physical stimuli for controlled delivery could lead to new therapeutic approaches.

6. Biosensing

Lanthanides are components in many biosensors: both emission-based and mass spectrometry (MS)-based bioassays have been extensively employed.

a. Emission-based Bioassays

Emission-based bioassays rely on fluorescence/luminescence for detection. They can be broadly divided into two categories – heterogeneous and homogeneous bioassays. Heterogeneous assays feature high affinity binding to target analytes through the use of capture molecules immobilized on a solid substrate. Notably, Ln^{3+}-doped UCNPs have been investigated for the detection of analytes due to the elimination of interference from background autofluorescence of biological cells and tissues.[33] Photostable single-band UCNPs (sb-UCNPs) were used to determine the expression levels of three biomarkers (estrogen receptors, progesterone receptors and human epithelial growth factor receptor-2) in breast cancer cells and tissue specimens via photoluminescence (PL), western blotting, immunocytochemistry (ICC), and immunohistochemistry (IHC).[48] Excellent correlations between sb-UCNP molecular profiling technology and ICC/IHC for protein expression in cell lines and biopsies (Figures 8a-b) were demonstrated, indicating that this new technology is a promising alternative for the multiplexed quantification of multiple tumor biomarkers. Other reports using Ln^{3+}-doped nanoparticles as bioprobes include the detection of additional tumor biomarkers such as urokinase plasminogen activator receptor, carcinoembryonic antigen; the recognition of a mucin-like protein expressed on human breast cancer MCF-7 cells by lanthanide binuclear helicate-avidin conjugates, and the detection of lysophosphatidic acid (a biomarker for ovarian cancer and other gynecologic cancers) by a methanol suspension of a Tb^{3+} and Eu^{3+} mixed-crystal metal-organic framework.[49,50,51,52]

In contrast to heterogeneous bioassays, homogeneous bioassays are largely based on the principles of Förster resonance energy transfer (FRET) for detection of protein-protein interactions, where long-range dipole–dipole interactions facilitate energy transfer between an excited donor molecule on one protein and a nearby acceptor molecule on another protein. Because of the suitability of lanthanide nanoparticles as FRET donors, including the inherently large Stokes shift of lanthanide systems that allows excitation at much shorter wavelengths than acceptor absorptions,[53] these nanoparticles have found their way into many homogeneous assays. Wang and coworkers[54] have designed a novel upconversion phosphor (UCP)-FRET biosensor for the detection of a cancer biomarker, matrix metalloproteinase-2, by using polyethylenimine-modified $NaYF_4$:Yb/Er UCPs and carbon nanoparticles as donor-acceptor pairs.

Many emission-based assays highlighted in this section also can be employed as time-resolved (TR) luminescent-based assays. Upon pulsed excitation of the lanthanide labels in lanthanide chelates and lanthanide-doped nanocrystals, the long-lived PL signal within an appropriate gate time is retained while the short-lived background noise is impeded within the delay time.[55] Due to high signal-to-noise ratios and detection sensitivities, TR fluoroimmunoassays using Ln^{3+}-chelates have been commercialized.[56] Heterogeneous TRPL assays and homogeneous TR-FRET assays also have been used to detect a variety of biomarkers and biomolecules, including the soluble urokinase plasminogen activator receptor with an impressive limit of detection of ~328 pM (similar to that found in the serum levels of cancer patients).[56-57] Several comprehensive reviews are available that cover this important area.[55,58,59,60]

b. Mass Spectrometry-based Bioassays

A combination of lanthanide labels and MS techniques has been used to detect a wide variety of nucleic acid and protein cancer biomarkers. Methods to multiplex proteins in FFPE tumor tissues using antibodies labeled with isotopic lanthanides and detection using secondary ion mass spectrometry have been developed.[61] Inductively coupled plasma MS (ICP-MS)-based analysis of lanthanide-labeled compounds has several advantages: (1) greater signal to noise due to the negligible natural biological abundance of lanthanides; (2) polyatomic interferences are rarely significant; (3) high ionization efficiency due to low first ionization potentials; (4) similar chemical properties suitable for multiplexed assays based on ICP-MS, and (5) potential for quantification using isotope dilution.[62] In a comprehensive review by de Bang and coworkers, applications of lanthanide-labeled proteins, nucleic acids, and ICP-MS in immunoassays and hybridization assays were covered in detail.[62]

Although methods for nucleic-acid detection using lanthanide labeled probes are still in their infancy, there have been steady developments in this area over recent years. One recent example demonstrated the detection of *Arabidopsis thaliana* microRNAs (miRNAs) on Northern blot membranes by laser ablation inductively coupled plasma mass spectrometry using ^{165}Ho, ^{159}Tb, and ^{169}Tm-labeled complementary DNA probes (Figure 9).[63] Following this proof-of-concept, it would be of interest to investigate the use of such probes to detect miRNA biomarkers and circulating tumor DNA for early cancer diagnosis.

c. Drug Design

It is well established that molecular interactions in solution can be followed by nuclear magnetic resonance (NMR) spectroscopy. In work exploiting NMR, a Dy^{3+} or Tm^{3+}-conjugated carbohydrate ligand was used to observe binding to the human galectin-3 carbohydrate recognition domain via pseudocontact shifts arising from the transfer of paramagnetic lanthanide signals to protein nuclei.[64] This method has potential applications for screening ligand-protein interactions, finding target sites for cancer drug discovery, and aiding in drug design.

Lanthanide ions, including Lu^{3+} and Tb^{3+}, also have been employed for protein crystal structure determination.[65,66] Two Tb^{3+}-binding modules connected to a 32-residue peptide tagged to ubiquitin were used for accurate structure determination by a single-wavelength

anomalous diffraction method, thereby eliminating the need for unnatural amino acids or some other chemical modification of the protein (Figure 10).[65] Tagging proteins with fusion peptides helps solve the phase problem, owing to robust anomalous signals from Ln ions, thereby offering structural biologists another powerful method for the determination of cancer-implicated protein structures required for inhibitor design.

7. Bioimaging

Lanthanides have been extensively employed as bioimaging agents for cancer diagnosis and treatment. In this section, lanthanides for MRI, NIR emission imaging, dual-/multi-mode imaging, IGT, and time-resolved luminescence imaging will be discussed briefly. For more in depth coverage, reviews on bioimaging applications using lanthanide nanoparticles are recommended.[29, 67]

a. Magnetic Resonance Imaging

Among the lanthanide ions, Gd^{3+} is especially suitable as a contrast agent, owing to its paramagnetism (with seven unpaired 4f electrons) and long electronic relaxation time. It is an ideal lanthanide ion for longitudinal T_1 relaxation enhancement. As uncomplexed Gd^{3+} is cytotoxic, it is normally used in chelated form (two examples are the well-known gadopentetic acid and gadoteric acid or encapsulated in nanomaterials, including nanocrystals, nanoparticles, and carbon nanostructures).[68] Other lanthanide ions such as Eu^{3+}, Dy^{3+}, and Er^{3+} that possess asymmetric electronic ground states, strong magnetic anisotropy, short electronic relaxation times, and large magnetic moments have been investigated as nanoparticle--based contrast agents in T_2-weighted MRI.[29,69]

b. Near-infrared Excitation-based Imaging

UCNPs can combine two or more lower energy photons to generate a single high-energy photon by an anti-Stokes process.[70] As a result, lanthanide-doped UCNPs have been extensively investigated in recent years as NIR imaging agents due to their excellent photostability, continuous emission capability, sharp multi-peak line emission, and long luminescence decay times (much longer than those of organic dyes and quantum dots).[70] In addition, light scattering by biological tissues is substantially reduced with NIR excitation, resulting in greater penetration depth than possible with UV-vis excitation. One example is the *in vivo* luminescence imaging of tumors by hexagonal phase $NaYF_4$:Yb,Er/$NaGdF_4$ core-shell UCNPs conjugated with Ce6 as contrast agents (Figure 11).[32]

c. Dual-/Multi-mode Imaging

Dual-/multi-mode imaging is becoming increasingly attractive as it combines the advantages of penetration depth, resolution, and sensitivity of different modalities, thereby providing more information than can be obtained from a single technique. Most reports of dual-/multi-modal imaging describe the application of lanthanide nanomaterials rather than lanthanide complexes due to their greater versatility and ease of preparation. The most common nanomaterials reported are, unexpectedly, lanthanide-doped UCNPs, which have found their way into a myriad of imaging modalities, including dual T_2-weighted MRI and upconversion luminescence imaging,[71] and *in vivo* four-modal imaging (upconversion luminescence

imaging, X-ray computed tomography, MRI, and single-photon emission computed tomography).[72]

d. Image-guided Therapy

As noted in previous sections (PDT, XRT, and drug/gene delivery), the incorporation of lanthanides into nanosystems and complexes serves a key purpose for IGT. IGT is important for the accurate determination of location and treatment of tumor sites. Specifically, lanthanide-doped UCNPs convert NIR excitation energy into UV-vis luminescence used to photorelease drugs and monitor their delivery. Previously reported applications include the photoisomerization driven release of doxorubicin[73] – as $NaYF_4$:TmYb@$NaYF_4$ UCNPs emit photons in the UV-vis region upon irradiation by NIR light, the azo moieties in the silica layer interconvert reversibly between cis and trans conformations (Figure 12a) and act as molecular impellers driving the release of encapsulated doxorubicin from silica mesopores (Figure 12b).

e. Time-resolved Luminescence Imaging

This imaging technique involves time-resolved luminescence microscopy (TRLM) and Ln^{3+} tags for cancer cell imaging.[74] TRLM is able to eliminate short-lifetime (< 100 ns) autofluorescence background from biological specimens and overcome the low photon emission from lanthanide probes by employing light-emitting diodes for pulsed epi-illumination and intensified charge-coupled device cameras for gated, widefield detection.[75] For example, self-assembled Eu^{3+} bimetallic helicates ($Eu_2(L^{C5})_3$) were found to localize into endosomes and/or lysosomes of HeLa cells by a combination of bright-field microscopy and TRLM (Figure 13).[76]

The development of new technologies and lanthanide tags for TRLM is advancing rapidly;[77] in this area, recent investigations employing time-resolved confocal microscopy[78] and time-resolved orthogonal scanning automated microscopy are of wide interest.[79]

8. Concluding Remarks and Future Outlook

As the worldwide incidence of cancer continues to rise, the discovery and continual refinement of diagnostics and therapeutics remain ongoing challenges. Increased availabilities of lanthanide compounds with outstanding stability (photo- and redox-stability) and luminescent properties have led to myriad applications in cancer therapy and imaging – as cytotoxic agents, inhibitors; in PDT, XRT, drug/gene delivery, biosensing, and bioimaging. Together with the utilization of lanthanide-based conjugates of biopolymers, it is likely that multi-modal IGT will be an attractive approach, as drugs can be released on demand via environmental stimuli and uptake can be accurately monitored, allowing for great specificity in tumor targeting.

Immunotherapeutics often have been heralded as the future of cancer medicine.[80] Therefore, another key area of development involves nanoparticle-based strategies that incorporate immune potentiators and α-emitters as a new-generation of lanthanide-based RIT agents. Immune potentiators function as vaccine adjuvants while α-emitters, as previously discussed, leave healthy cells unaffected by radiation.

Lastly, owing to the recently discovered potential of adoptive cell transfer in treating a wide variety of cancers,[81] lanthanide-based labeling of chimeric antigen receptor T-cells for real-time biotracking and bioimaging is a promising avenue for exploration, as there is great therapeutic potential in this area.

Acknowledgments

Funding Sources

This work was supported by the Caltech-City of Hope Biomedical Research Initiative (J.T. and H.B.G.) and the AACR Thomas J. Bardos Science Education Award (R.D.T.). Support from NIH R01 DK019038 (H.B.G.) and NIH R01 CA176611 (J.T.) also are acknowledged.

Biography

Ruijie D. Teo (Darius) was born in Singapore and graduated with B.S. and M.S. degrees in Chemistry at Caltech. He was actively involved in developing metal-based anti-cancer drugs during his time at Caltech under Professor Harry B. Gray and Professor John Termini. He is a recipient of the American Association for Cancer Research (AACR) Thomas J. Bardos Science Education Award and plans to attend graduate school in the fall of 2016.

John Termini was born and raised in New York, and received his B.A., M.S., M.Phil. and Ph.D. degrees in Chemistry at Columbia University. His graduate research was in natural products synthesis and biochemistry under Professor Koji Nakanishi. He went on to become an American Cancer Society postdoctoral fellow at Caltech in the laboratory of Professor Peter B. Dervan. He is currently a Professor in the Department of Molecular Medicine at the Beckman Research Institute of City of Hope in Duarte CA. His research interests include the role of DNA damage and repair in human diseases and the therapeutic applications of metal-containing drugs in cancer and diabetes.

Harry B. Gray completed a doctoral thesis on inorganic reaction mechanisms at Northwestern University. He developed ligand field theory as a postdoctoral fellow at the University of Copenhagen before joining the chemistry faculty at Columbia University, where in the early 1960s he investigated the electronic structures of metal complexes. He moved to Caltech in 1966, where he is the Arnold O. Beckman Professor of Chemistry and the Founding Director of the Beckman Institute. A Wolf Prize Laureate, his work on long-range electron transfer through proteins has led to profound changes in the understanding of biological electron flow and energy transduction.

ABBREVIATIONS

CDK4	cyclin-dependent kinase 4
Ce6	chlorin e6
DNA	deoxyribonucleic acid
FDA	Food and Drug Administration
FFPE	formaldehyde fixed-paraffin embedded

FRET	Förster resonance energy transfer
ICP-MS	inductively coupled plasma mass spectrometry
IGT	image-guided therapy
ICC	immunocytochemistry
IHC	immunohistochemistry
ISC	intersystem crossing
MAPK	mitogen-activated protein kinases
miRNA	micro-ribonucleic acid
MRI	magnetic resonance imaging
MS	mass-spectrometry
NIR	near-infrared
NMR	nuclear magnetic resonance
PDT	photodynamic therapy
PL	photoluminescence
Plk1	polo-like kinase 1
PMSA	prostate-specific membrane antigen
RIT	radioimmunotherapy
RNA	ribonucleic acid
ROS	reactive oxygen species
sb-UCNP	single-band upconversion nanoparticle
TR	time-resolved
TRLM	time-resolved luminescence microscopy
UCNP	upconversion nanoparticle
UCP	upconversion phosphor
UV	ultraviolet
UV-vis	ultraviolet-visible
XRT	radiation therapy

REFERENCES

1. Tauxe W. A Tumour Through Time. Nature. 2015; 527:S102–S103. [PubMed: 26580155]

2. The Cancer Atlas. [Dec 21, 2015] History of Cancer. canceratlas.cancer.org/history-cancer/
3. Siegel RL, Miller KD, Jemal A. Cancer Statistics, 2015. CA: Cancer J. Clin. 2015; 65:339–344. [PubMed: 26208318]
4. Beatty, R. The Lanthanides. Marshall Cavendish; Tarrytown, NY: 2008. p. 10
5. Bünzli J-CG. On the Design of Highly Luminescent Lanthanide Complexes. Coord. Chem. Rev. 2015; 293–294:19–47.
6. Magerstädt M, Gansow OA, Brechbiel MW, Colcher D, Baltzer L, Knop RH, Girton ME, Naegele M. Gd(DOTA): An Alternative to Gd(DTPA) as a T1,2 Relaxation Agent for NMR Imaging or Spectroscopy. Magn. Reson. Med. 1986; 3:808–812. [PubMed: 3784897]
7. Larson SM, Carrasquillo JA, Cheung N-KV, Press OW. Radioimmunotherapy of Human Tumours. Nat. Rev. Cancer. 2015; 15:347–360. [PubMed: 25998714]
8. Park JY, Chang Y, Lee GH. Multi-Modal Imaging and Cancer Therapy Using Lanthanide Oxide Nanoparticles: Current Status and Perspectives. Curr. Med. Chem. 2015; 22:569–581. [PubMed: 25439587]
9. Karakoti AS, Monteiro-Riviere NA, Aggarwal R, Davis JP, Narayan RJ, Self WT, McGinnis J, Seal S. Nanoceria as Antioxidant: Synthesis and Biomedical Applications. JOM. 2008; 60:33–37. [PubMed: 20617106]
10. Anghileri LJ, Crone-Escanye MC, Robert J. Antitumor Activity of Gallium and Lanthanum: Role of Cation-Cell Membrane Interaction. Anticancer Res. 1987; 7:1205–1208. [PubMed: 2964807]
11. Kostova I, Manolov I, Konstantinov S, Karaivanova M. Synthesis, Physicochemical Characterisation and Cytotoxic Screening of New Complexes of Cerium, Lanthanum and Neodymium with Warfarin and Coumachlor Sodium Salts. Eur. J. Med. Chem. 1999; 34:63–68.
12. Chen Z-F, Song X-Y, Peng Y, Hong X, Liu Y-C, Liang H. High Cytotoxicity of Dihalo-Substituted 8-Quinolinolato-Lanthanides. Dalton Trans. 2011; 40:1684–1692. [PubMed: 21258737]
13. Fricker SP. The Therapeutic Application of Lanthanides. Chem. Soc. Rev. 2006; 35:524–533. [PubMed: 16729146]
14. Liu Y-C, Chen Z-F, Song X-Y, Peng Y, Qin Q-P, Liang H. Synthesis, Crystal Structure, Cytotoxicity and DNA Interaction of 5,7-Dibromo-8-Quinolinolato-Lanthanides. Eur. J. Med. Chem. 2013; 59:168–175. [PubMed: 23220645]
15. Wei J-H, Chen Z-F, Qin J-L, Liu Y-C, Li Z-Q, Khan T-M, Wang M, Jiang Y-H, Shen W-Y, Liang H. Water-Soluble Oxoglaucine-Y(III), Dy(III) Complexes: In Vitro and In Vivo Anticancer Activities by Triggering DNA Damage, Leading to S Phase Arrest and Apoptosis. Dalton Trans. 2015; 44:11408–11419. [PubMed: 26017376]
16. Reed KC, Bygrave FL. The Inhibition of Mitochondrial Calcium Transport by Lanthanides and Ruthenium Red. Biochem. J. 1974; 140:143–155. [PubMed: 4375957]
17. Kwong W-L, Wai-Yin Sun R, Lok C-N, Siu F-M, Wong S-Y, Low K-H, Che C-M. An Ytterbium(III) Porphyrin Induces Endoplasmic Reticulum Stress and Apoptosis in Cancer Cells: Cytotoxicity and Transcriptomics Studies. Chem. Sci. 2013; 4:747–754.
18. Citta A, Folda A, Scutari G, Cesaro L, Bindoli A, Rigobello MP. Inhibition of Thioredoxin Reductase by Lanthanum Chloride. J. Inorg. Biochem. 2012; 117:18–24. [PubMed: 23078771]
19. Magda D, Lecane P, Miller RA, Lepp C, Miles D, Mesfin M, Biaglow JE, Ho VV, Chawannakul D, Nagpal S, Karaman MW, Hacia JG. Motexafin Gadolinium Disrupts Zinc Metabolism in Human Cancer Cell Lines. Cancer Res. 2005; 65:3837–3845. [PubMed: 15867382]
20. Wason MS, Zhao J. Cerium Oxide Nanoparticles: Potential Applications for Cancer and Other Diseases. Am. J. Transl. Res. 2013; 5:126–131. [PubMed: 23573358]
21. Cheng G, Guo W, Han L, Chen E, Kong L, Wang L, Ai W, Song N, Li H, Chen H. Cerium Oxide Nanoparticles Induce Cytotoxicity in Human Hepatoma SMMC-7721 Cells via Oxidative Stress and the Activation of MAPK Signaling Pathways. Toxicol. In Vitro. 2013; 27:1082–1088. [PubMed: 23416263]
22. Chan C-F, Xie C, Tsang M-K, Lear S, Dai L, Zhou Y, Cicho J, Karbowiak M, Hreniak D, Lan R, Cobb SL, Lam MH-W, Hao J, Wong K-L. The Effects of Morphology and Linker Length on the Properties of Peptide–Lanthanide Upconversion Nanomaterials as G2 Phase Cell Cycle Inhibitors. Eur. J. Inorg. Chem. 2015; 2015:4539–4545.

23. Chan C-F, Tsang M-K, Li H, Lan R, Chadbourne FL, Chan W-L, Law G-L, Cobb SL, Hao J, Wong W-T, Wong K-L. Bifunctional Up-Converting Lanthanide Nanoparticles for Selective In Vitro Imaging and Inhibition of Cyclin D as Anti-Cancer Agents. J. Mater. Chem. B. 2014; 2:84–91.
24. Beck A, Reichert JM. Antibody-Drug Conjugates. mAbs. 2014; 6:15–17. [PubMed: 24423577]
25. Josefsen LB, Boyle RW. Photodynamic Therapy and the Development of Metal-Based Photosensitizers. Met.-Based Drugs. 2008; 2008:276109. [PubMed: 18815617]
26. Sessler JL, Dow WC, O'Connor D, Harriman A, Hemmi G, Mody TD, Miller RA, Qing F, Springs S, Woodburn K, Young SW. Biomedical Applications of Lanthanide (III) Texaphyrins Lutetium(III) Texaphyrins as Potential Photodynamic Therapy Photosensitizers. J. Alloys Compd. 1997; 249:146–152.
27. Zhang T, Chan C-F, Hao J, Law G-L, Wong W-K, Wong K-L. Fast Uptake, Water-Soluble, Mitochondria-Specific Erbium Complex for a Dual Function Molecular Probe - Imaging and Photodynamic Therapy. RSC Adv. 2013; 3:382–385.
28. Zhang T, Lan R, Chan C-F, Law G-L, Wong W-K, Wong K-L. In Vivo Selective Cancer-Tracking Gadolinium Eradicator as New-Generation Photodynamic Therapy Agent. Proc. Natl. Acad. Sci. U.S.A. 2014; 111:E5492–E5497. [PubMed: 25453097]
29. Dong H, Du S-R, Zheng X-Y, Lyu G-M, Sun L-D, Li L-D, Zhang P-Z, Zhang C, Yan C-H. Lanthanide Nanoparticles: From Design Toward Bioimaging and Therapy. Chem. Rev. 2015; 115:10725–10815. [PubMed: 26151155]
30. Zheng W, Huang P, Tu D, Ma E, Zhu H, Chen X. Lanthanide-Doped Upconversion Nano-Bioprobes: Electronic Structures, Optical Properties, and Biodetection. Chem. Soc. Rev. 2015; 44:1379–1415. [PubMed: 25093303]
31. Wang M, Chen Z, Zheng W, Zhu H, Lu S, Ma E, Tu D, Zhou S, Huang M, Chen X. Lanthanide-Doped Upconversion Nanoparticles Electrostatically Coupled with Photosensitizers for Near-Infrared-Triggered Photodynamic Therapy. Nanoscale. 2014; 6:8274–8282. [PubMed: 24933297]
32. Park YI, Kim HM, Kim JH, Moon KC, Yoo B, Lee KT, Lee N, Choi Y, Park W, Ling D, Na K, Moon WK, Choi SH, Park HS, Yoon S-Y, Suh YD, Lee SH, Hyeon T. Theranostic Probe Based on Lanthanide-Doped Nanoparticles for Simultaneous In Vivo Dual-Modal Imaging and Photodynamic Therapy. Adv. Mater. 2012; 24:5755–5761. [PubMed: 22915170]
33. Tu D, Zheng W, Liu Y, Zhu H, Chen X. Luminescent Biodetection Based on Lanthanide-Doped Inorganic Nanoprobes. Coord. Chem. Rev. 2014; 273–274:13–29.
34. Liu Y, Chen W, Wang S, Joly AG, Westcott S, Woo BK. X-ray Luminescence of LaF_3:Tb^{3+} and LaF_3:Ce^{3+},Tb^{3+} Water-Soluble Nanoparticles. J. Appl. Phys. 2008; 103:063105.
35. Kaščáková S, Giuliani A, Lacerda S, Pallier A, Mercère P, Tóth É, Réfrégiers M. X-ray-Induced Radiophotodynamic Therapy (RPDT) Using Lanthanide Micelles: Beyond Depth Limitations. Nano Res. 2015; 8:2373–2379.
36. Bulin A-L, Truillet C, Chouikrat R, Lux F, Frochot C, Amans D, Ledoux G, Tillement O, Perriat P, Barberi-Heyob M, Dujardin C. X-ray-Induced Singlet Oxygen Activation with Nanoscintillator-Coupled Porphyrins. J. Phys. Chem. C. 2013; 117:21583–21589.
37. Fountain, ME. Ph.D. Thesis. Austin: Aug. 2008 Synthesis and Studies of Gadolinium Texaphyrin Conjugates and Model Platinum Therapeutic Agents..
38. Tagawa ST, Beltran H, Vallabhajosula S, Goldsmith SJ, Osborne J, Matulich D, Petrillo K, Parmar S, Nanus DM, Bander NH. Anti–Prostate-Specific Membrane Antigen-Based Radioimmunotherapy for Prostate Cancer. Cancer. 2010; 116:1075–1083. [PubMed: 20127956]
39. Berndt C, Kurz T, Bannenberg S, Jacob R, Holmgren A, Brunk UT. Ascorbate and Endocytosed Motexafin Gadolinium Induce Lysosomal Rupture. Cancer Lett. 2011; 307:119–123. [PubMed: 21492999]
40. Donnelly ET, Liu Y, Paul TK, Rockwell S. Effects of Motexafin Gadolinium on DNA Damage and X-ray-Induced DNA Damage Repair, as Assessed by the Comet Assay. Int. J. Radiat. Oncol. Biol. Phys. 2005; 62:1176–1186. [PubMed: 15990023]
41. Dehnad H, Kal HB, Stam T, Gademan IS, van Moorselaar RJA, van der Sanden BPJ. Response to Motexafin Gadolinium and Ionizing Radiation of Experimental Rat Prostate and Lung Tumors. Int. J. Radiat. Oncol. Biol. Phys. 2003; 57:787–793. [PubMed: 14529785]

42. Jacobs SA. (90)Yttrium Ibritumomab Tiuxetan in the Treatment of Non-Hodgkin's Lymphoma: Current Status and Future Prospects. Biologics: Targets & Therapy. 2007; 1:215–227. [PubMed: 19707332]
43. Alcindor T, Witzig T. Radioimmunotherapy with Yttrium-90 Ibritumomab Tiuxetan for Patients with Relapsed CD20+ B-Cell Non-Hodgkin's Lymphoma. Curr. Treat. Options in Oncol. 2002; 3:275–282.
44. McLaughlin MF, Woodward J, Boll RA, Wall JS, Rondinone AJ, Kennel SJ, Mirzadeh S, Robertson JD. Gold Coated Lanthanide Phosphate Nanoparticles for Targeted Alpha Generator Radiotherapy. PLoS ONE. 2013; 8:e54531. [PubMed: 23349921]
45. Palmer GD, Stoddart MJ, Gouze E, Gouze JN, Ghivizzani SC, Porter RM, Evans CH. A Simple, Lanthanide-Based Method to Enhance the Transduction Efficiency of Adenovirus Vectors. Gene Ther. 2008; 15:357–363. [PubMed: 18283289]
46. Zhang X, Ge J, Xue Y, Lei B, Yan D, Li N, Liu Z, Du Y, Cai R. Controlled Synthesis of Ultrathin Lanthanide Oxide Nanosheets and Their Promising pH-Controlled Anticancer Drug Delivery. Chem. Euro. J. 2015; 21:11954–11960.
47. Shen J, Zhao L, Han G. Lanthanide-Doped Upconverting Luminescent Nanoparticle Platforms for Optical Imaging-Guided Drug Delivery and Therapy. Adv. Drug Deliv. Rev. 2013; 65:744–755. [PubMed: 22626980]
48. Zhou L, Wang R, Yao C, Li X, Wang C, Zhang X, Xu C, Zeng A, Zhao D, Zhang F. Single-Band Upconversion Nanoprobes for Multiplexed Simultaneous In Situ Molecular Mapping of Cancer Biomarkers. Nat. Commun. 2015; 6:6938. [PubMed: 25907226]
49. Liu Y, Tu D, Zhu H, Chen X. Lanthanide-Doped Luminescent Nanoprobes: Controlled Synthesis, Optical Spectroscopy, and Bioapplications. Chem. Soc. Rev. 2013; 42:6924–6958. [PubMed: 23775339]
50. Fernandez-Moreira V, Song B, Sivagnanam V, Chauvin A-S, Vandevyver CDB, Gijs M, Hemmila I, Lehr H-A, Bünzli J-CG. Bioconjugated Lanthanide Luminescent Helicates as Multilabels for Lab-On-A-Chip Detection of Cancer Biomarkers. Analyst. 2010; 135:42–52. [PubMed: 20024180]
51. Chen, X.; Liu, Y.; Tu, D. Lanthanide-Doped Luminescent Nanomaterials. Springer; Heidelberg: 2014. p. 130
52. Zhang S-Y, Shi W, Cheng P, Zaworotko MJ. A Mixed-Crystal Lanthanide Zeolite-like Metal–Organic Framework as a Fluorescent Indicator for Lysophosphatidic Acid, a Cancer Biomarker. J. Am. Chem. Soc. 2015; 137:12203–12206. [PubMed: 26355993]
53. Geißler D, Linden S, Liermann K, Wegner KD, Charbonnière LJ, Hildebrandt N. Lanthanides and Quantum Dots as Förster Resonance Energy Transfer Agents for Diagnostics and Cellular Imaging. Inorg. Chem. 2014; 53:1824–1838. [PubMed: 24099579]
54. Wang Y, Shen P, Li C, Wang Y, Liu Z. Upconversion Fluorescence Resonance Energy Transfer Based Biosensor for Ultrasensitive Detection of Matrix Metalloproteinase-2 in Blood. Anal. Chem. 2012; 84:1466–1473. [PubMed: 22242647]
55. Zheng W, Tu D, Huang P, Zhou S, Chen Z, Chen X. Time-Resolved Luminescent Biosensing Based on Inorganic Lanthanide-Doped Nanoprobes. Chem. Commun. 2015; 51:4129–4143.
56. Zheng W, Zhou S, Chen Z, Hu P, Liu Y, Tu D, Zhu H, Li R, Huang M, Chen X. Sub-10 nm Lanthanide-Doped CaF_2 Nanoprobes for Time-Resolved Luminescent Biodetection. Angew. Chem. Int. Ed. 2013; 52:6671–6676.
57. Huai Q, Mazar AP, Kuo A, Parry GC, Shaw DE, Callahan J, Li Y, Yuan C, Bian C, Chen L, Furie B, Furie BC, Cines DB, Huang M. Structure of Human Urokinase Plasminogen Activator in Complex with Its Receptor. Science. 2006; 311:656–659. [PubMed: 16456079]
58. Bünzli J-CG. Lanthanide Luminescence for Biomedical Analyses and Imaging. Chem. Rev. 2010; 110:2729–2755. [PubMed: 20151630]
59. Yuan J, Wang G. Lanthanide-Based Luminescence Probes and Time-Resolved Luminescence Bioassays. Trends Anal. Chem. 2006; 25:490–500.
60. Hagan AK, Zuchner T. Lanthanide-Based Time-Resolved Luminescence Immunoassays. Anal. Bioanal. Chem. 2011; 400:2847–2864. [PubMed: 21556751]

61. Angelo M, Bendall SC, Finck R, Hale MB, Hitzman C, Borowsky AD, Levenson RM, Lowe JB, Liu SD, Zhao S, Natkunam Y, Nolan GP. Multiplexed Ion Beam Imaging of Human Breast Tumors. Nat. Med. 2014; 20:436–442. [PubMed: 24584119]
62. de Bang TC, Husted S. Lanthanide Elements as Labels for Multiplexed and Targeted Analysis of Proteins, DNA and RNA Using Inductively-Coupled Plasma Mass Spectrometry. Trends Anal. Chem. 2015; 72:45–52.
63. de Bang TC, Shah P, Cho SK, Yang SW, Husted S. Multiplexed microRNA Detection Using Lanthanide-Labeled DNA Probes and Laser Ablation Inductively Coupled Plasma Mass Spectrometry. Anal. Chem. 2014; 86:6823–6826. [PubMed: 24945747]
64. Canales Á, Mallagaray Á, Berbís MÁ, Navarro-Vázquez A, Domínguez G, Cañada FJ, André S, Gabius H-J, Pérez-Castells J, Jiménez-Barbero J. Lanthanide-Chelating Carbohydrate Conjugates Are Useful Tools To Characterize Carbohydrate Conformation in Solution and Sensitive Sensors to Detect Carbohydrate–Protein Interactions. J. Am. Chem. Soc. 2014; 136:8011–8017. [PubMed: 24831588]
65. Silvaggi NR, Martin LJ, Schwalbe H, Imperiali B, Allen KN. Double-Lanthanide-Binding Tags for Macromolecular Crystallographic Structure Determination. J. Am. Chem. Soc. 2007; 129:7114–71120. [PubMed: 17497863]
66. Pompidor G, Maury O, Vicat J, Kahn RA. Dipicolinate Lanthanide Complex for Solving Protein Structures Using Anomalous Diffraction. Acta Crystallogr. Sect. D. 2010; 66:762–769. [PubMed: 20606256]
67. Comby S, Surender EM, Kotova O, Truman LK, Molloy JK, Gunnlaugsson T. Lanthanide-Functionalized Nanoparticles as MRI and Luminescent Probes for Sensing and/or Imaging Applications. Inorg. Chem. 2014; 53:1867–1879. [PubMed: 24354305]
68. Ghiassi KB, Olmstead MM, Balch AL. Gadolinium-Containing Endohedral Fullerenes: Structures and Function as Magnetic Resonance Imaging (MRI) Agents. Dalton Trans. 2014; 43:7346–7358. [PubMed: 24522668]
69. Kattel K, Park JY, Xu W, Kim HG, Lee EJ, Bony BA, Heo WC, Lee JJ, Jin S, Baeck JS. A Facile Synthesis, In Vitro and In Vivo MR Studies of d-Glucuronic Acid-Coated Ultrasmall Ln_2O_3 (Ln = Eu, Gd, Dy, Ho, and Er) Nanoparticles as a New Potential MRI Contrast Agent. ACS Appl. Mater. Interfaces. 2011; 3:3325–3334. [PubMed: 21853997]
70. Han S, Deng R, Xie X, Liu X. Enhancing Luminescence in Lanthanide-Doped Upconversion Nanoparticles. Angew. Chem. Int. Ed. 2014; 53:11702–11715.
71. Cheng L, Yang K, Li Y, Chen J, Wang C, Shao M, Lee S-T, Liu Z. Facile Preparation of Multifunctional Upconversion Nanoprobes for Multimodal Imaging and Dual-Targeted Photothermal Therapy. Angew. Chem. Int. Ed. 2011; 50:7385–7390.
72. Sun Y, Zhu X, Peng J, Li F. Core–Shell Lanthanide Upconversion Nanophosphors as Four-Modal Probes for Tumor Angiogenesis Imaging. ACS Nano. 2013; 7:11290–11300. [PubMed: 24205939]
73. Liu J, Bu W, Pan L, Shi J. NIR-Triggered Anticancer Drug Delivery by Upconverting Nanoparticles with Integrated Azobenzene-Modified Mesoporous Silica. Angew. Chem. Int. Ed. 2013; 52:4375–4379.
74. Charbonnière L, Ziessel R, Guardigli M, Roda A, Sabbatini N, Cesario M. Lanthanide Tags for Time-Resolved Luminescence Microscopy Displaying Improved Stability and Optical Properties. J. Am. Chem. Soc. 2001; 123:2436–2437. [PubMed: 11456898]
75. Gahlaut N, Miller LW. Time-Resolved Microscopy for Imaging Lanthanide Luminescence in Living Cells. Cytometry A. 2010; 77A:1113–1125. [PubMed: 20824630]
76. Deiters E, Song B, Chauvin A-S, Vandevyver CDB, Gumy F, Bünzli J-CG. Luminescent Bimetallic Lanthanide Bioprobes for Cellular Imaging with Excitation in the Visible-Light Range. Chem. Euro. J. 2009; 15:885–900.
77. Montgomery CP, Murray BS, New EJ, Pal R, Parker D. Cell-Penetrating Metal Complex Optical Probes: Targeted and Responsive Systems Based on Lanthanide Luminescence. Acc. Chem. Res. 2009; 42:925–937. [PubMed: 19191558]
78. Liao Z, Tropiano M, Faulkner S, Vosch T, Sørensen TJ. Time-Resolved Confocal Microscopy Using Lanthanide Centred Near-IR Emission. RSC Adv. 2015; 5:70282–70286.

79. Lu Y, Lu J, Zhao J, Cusido J, Raymo FM, Yuan J, Yang S, Leif RC, Huo Y, Piper JA, Robinson JP, Goldys EM, Jin D. On-The-Fly Decoding Luminescence Lifetimes in the Microsecond Region for Lanthanide-Encoded Suspension Arrays. Nat. Commun. 2014; 5:3741. [PubMed: 24796249]

80. Schmidt C. Immunology: Another Shot at Cancer. Nature. 2015; 527:S105–S107. [PubMed: 26580157]

81. Fousek K, Ahmed N. The Evolution of T-Cell Therapies for Solid Malignancies. Clin. Cancer Res. 2015; 21:3384–3392. [PubMed: 26240290]

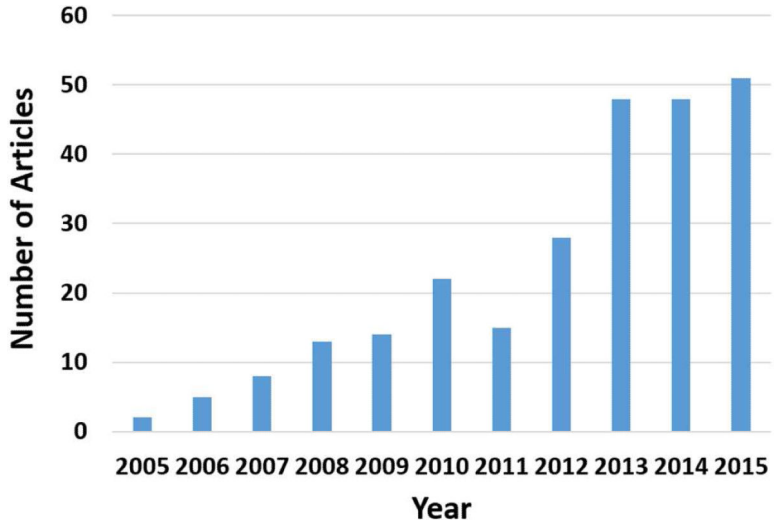

Figure 1.
Number of articles in *Web of Science* on the topic “lanthanide” and “cancer” from 2005 to 2015.

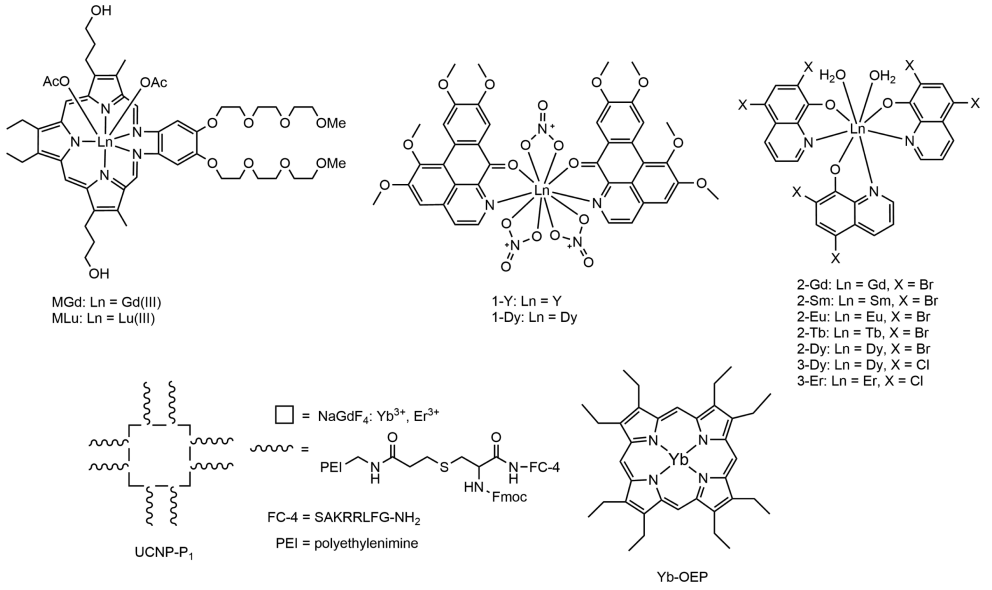

Scheme 1.

Structures of lanthanide-based molecules and nanoparticles that function as cytotoxic agents and inhibitors.

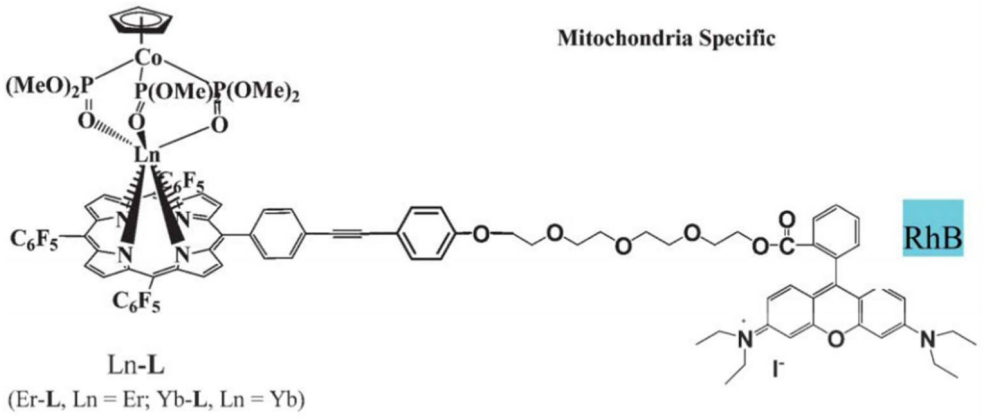

Figure 2.

Molecular structures of porphyrin-based lanthanide complexes, Er-L and Yb-L (Yb-L served as the control). Reproduced from ref. 27 with permission of the Royal Society of Chemistry.

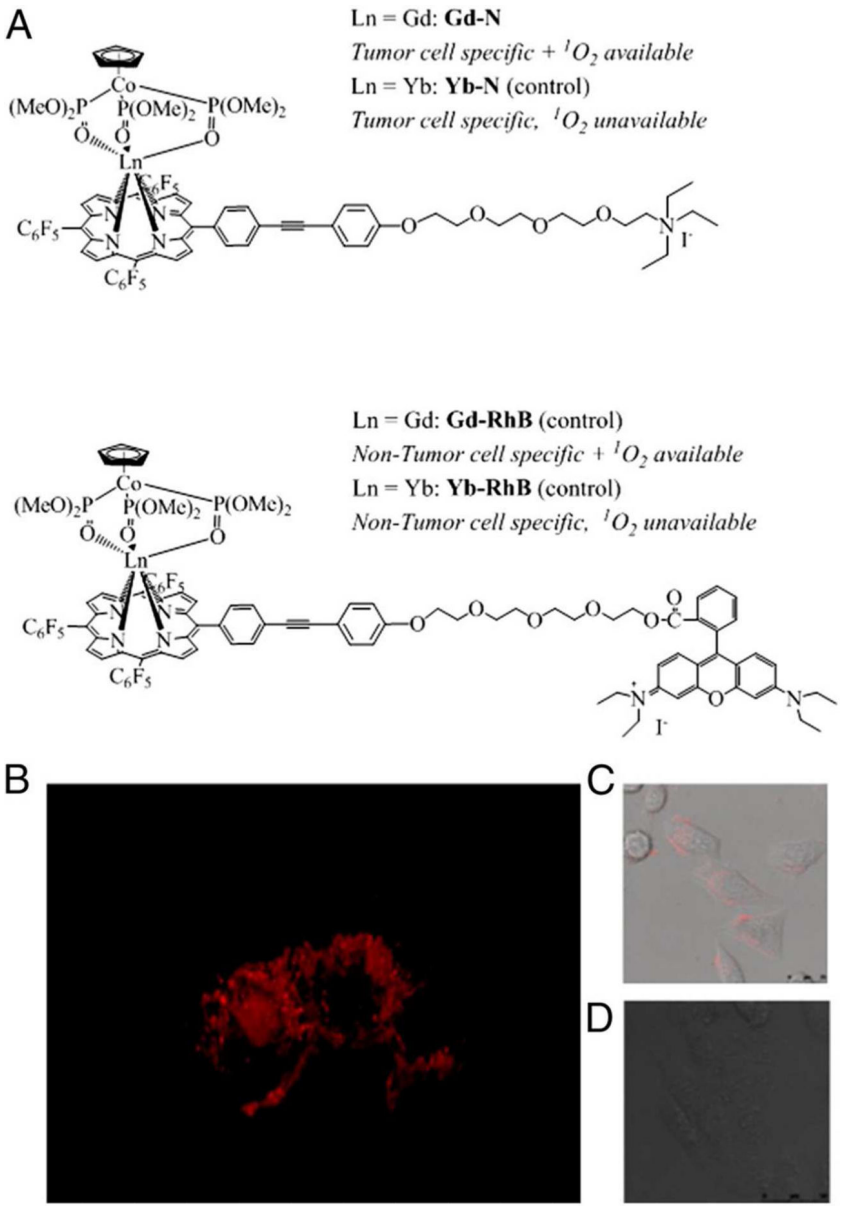

Figure 3.

a) Structure of “smart” cancer cell-specific PDT agent (Gd-N) and control analogs Yb-N and Gd-RhB. b) 3D in vitro imaging of Gd-N after 15-h incubation in HeLa cells. Subcellular localization of Gd-N in c) cancer cells (HeLa) and d) normal cells (WPMY-1). Reproduced with permission from ref. 28 (© 2014 National Academy of Sciences, USA).

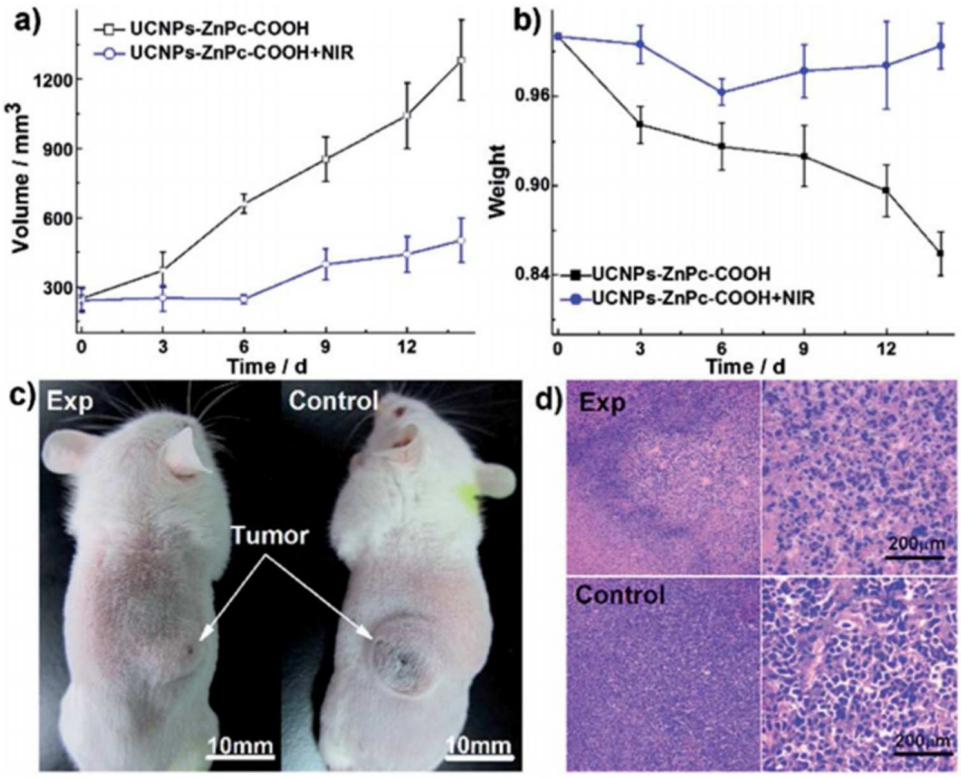

Figure 4.

Variation of (a) tumor volumes and (b) body weights of mice in experimental and control groups, respectively. Each data point represents the average value of 5 mice. (c) Representative photos of a mouse showing tumors at 14 days after treatment in experimental and control groups, respectively. (d) Images (left) and the corresponding high-resolution images (right) of hematoxylin–eosin stained tumor tissues harvested from the experimental and control groups after 14 days. Reproduced from ref. 31 with permission of the Royal Society of Chemistry.

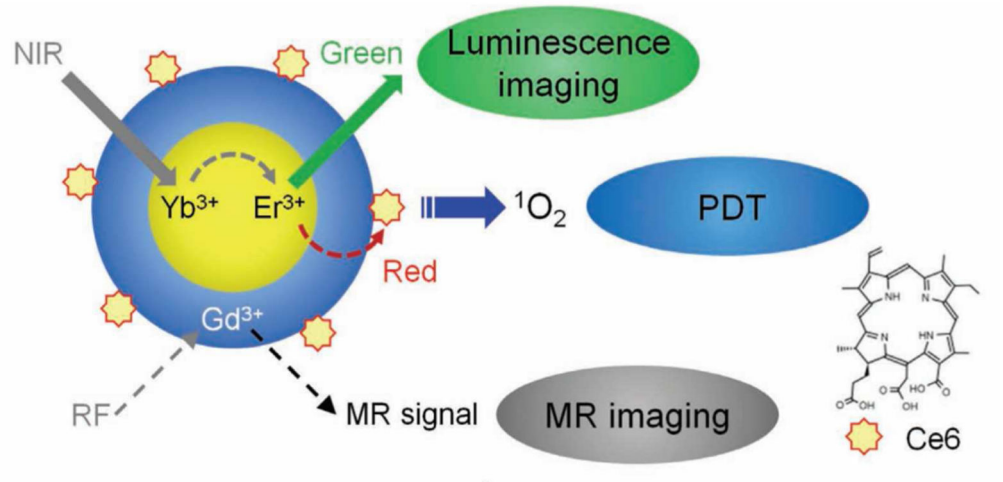

Figure 5.

Schematic of dual-modal imaging and PDT using UCNP–Ce6. Reproduced with permission from ref. 32 (© 2012 John Wiley & Sons Inc.).

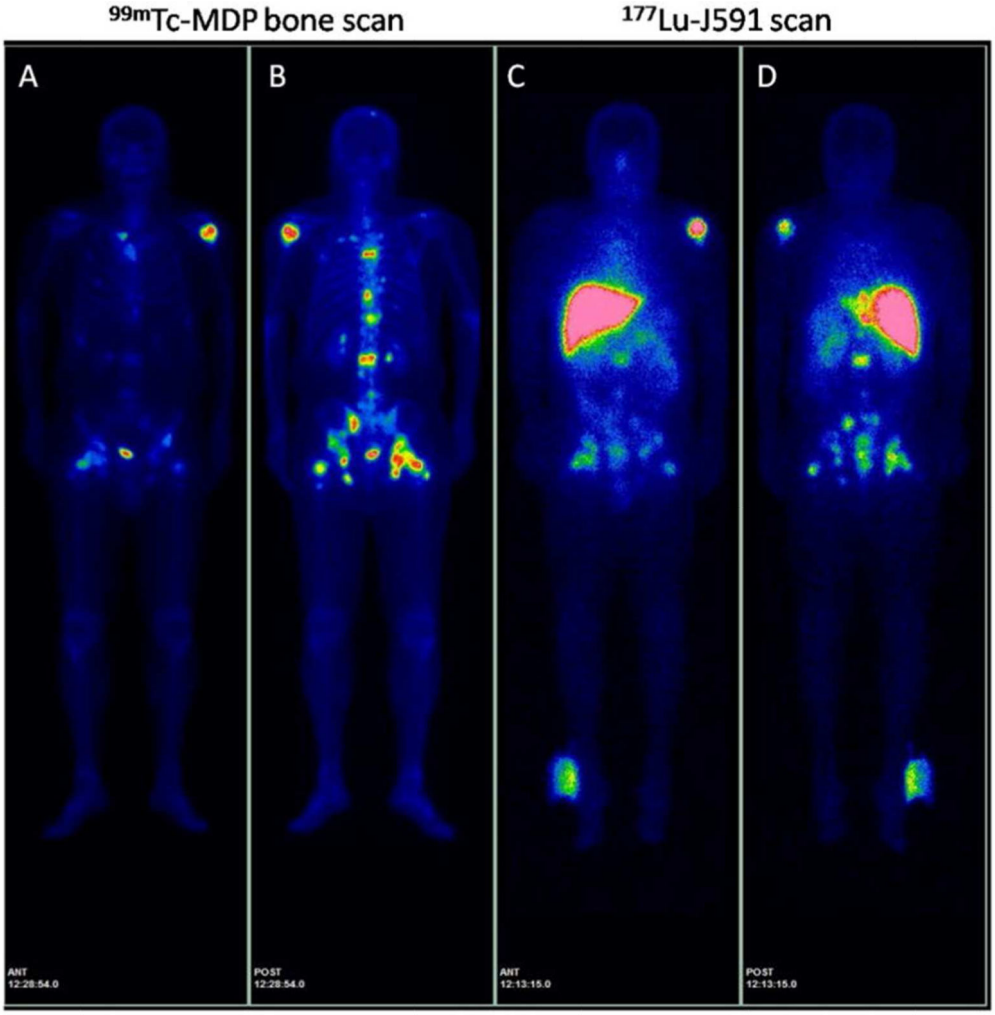

Figure 6.

Left panels: Anterior (A) and posterior (B) ^{99m}Tc-MDP bone scan images of pre- treatment bony metastases. Right panels: Anterior (C) and posterior (D) total body images obtained (via dual head gamma camera) of sites of uptake 7 days after ^{177}Lu-J591 administration. Note ^{177}Lu-J591 is cleared via the liver. Reproduced with permission from ref. 38 (© 2010 John Wiley & Sons Inc.).

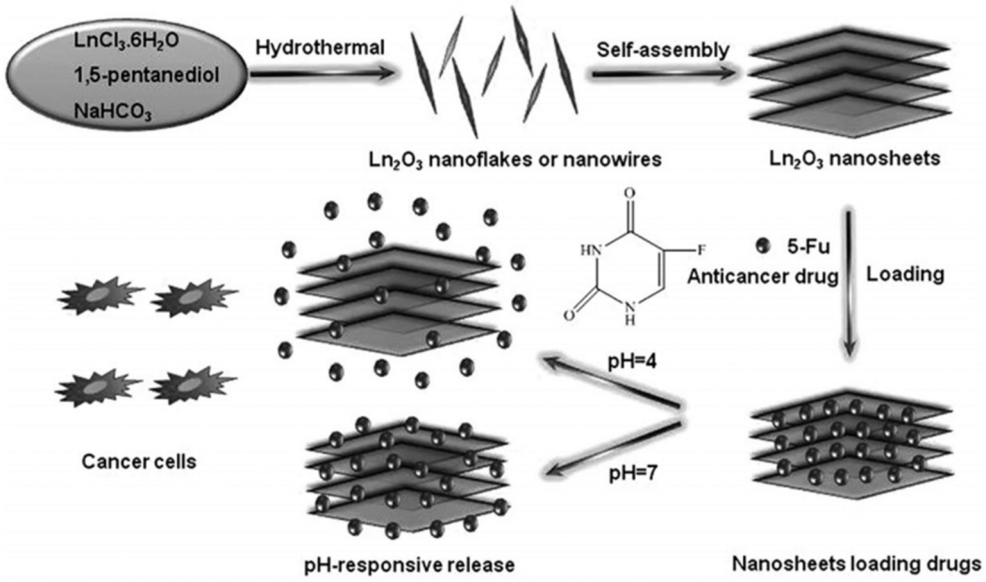

Figure 7.

Formation pathway for Sm_2O_3 and Gd_2O_3 nanostructures, as well as pH-controlled anticancer drug delivery. Reproduced with permission from ref. 46 (© 2015 John Wiley & Sons Inc.).

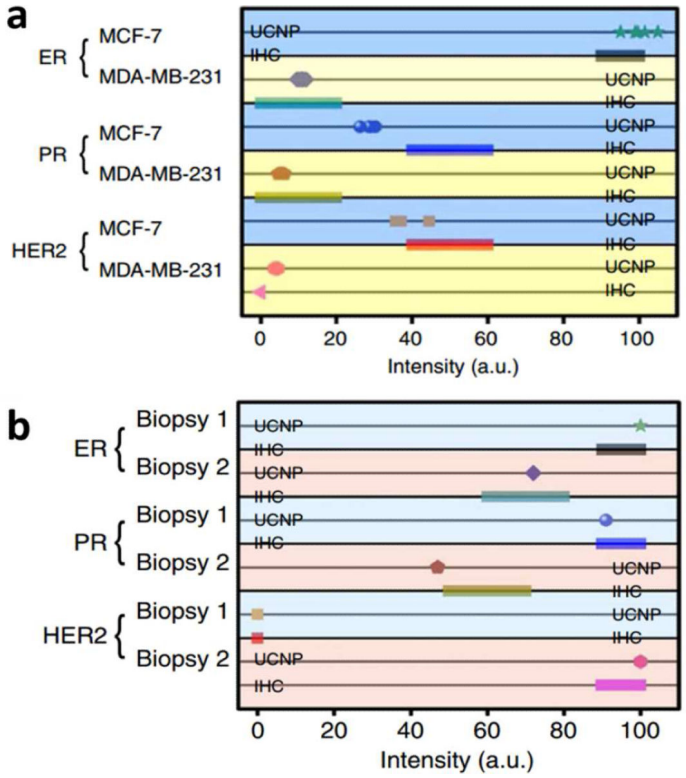

Figure 8.

Comparative statistical analysis of multiplexed detection with sb-UCNPs and IHC. (a) using two breast cancer cell-lines: MCF-7 and MDA-MB-231 (b) using three formaldehyde fixed-paraffin embedded (FFPE) human breast cancer tissues with primary antibodies-conjugated sb-UCNPs. Scale bar, 20 μm. Reproduced with permission from ref. 48 (© 2015 Nature Publishing Group).

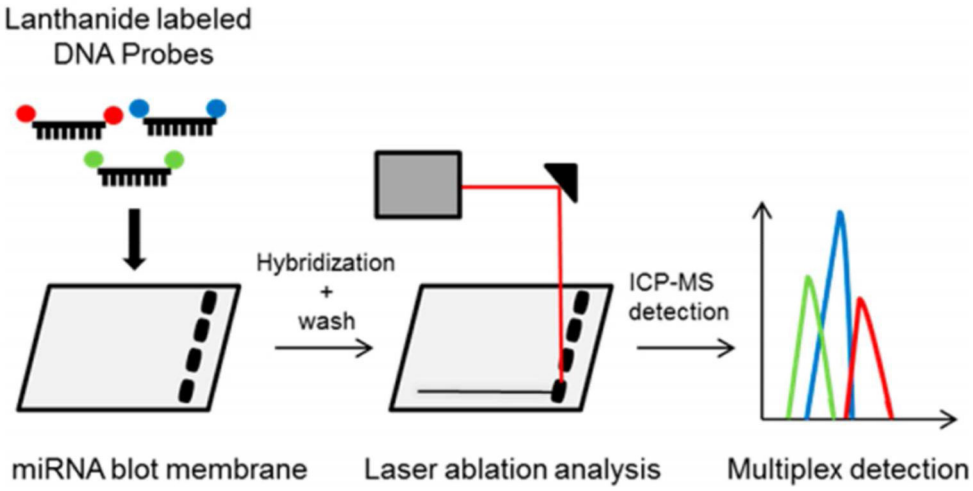

Figure 9.

miRNAs were northern blotted and incubated with lanthanide-labeled DNA probes. After hybridization and washing, the membrane was analyzed by laser ablation inductively coupled plasma mass spectrometry. The dry aerosol created by laser ablation was introduced to the ICP-MS for online detection of the lanthanide composition, thereby enabling multiplex detection of miRNAs.[63]

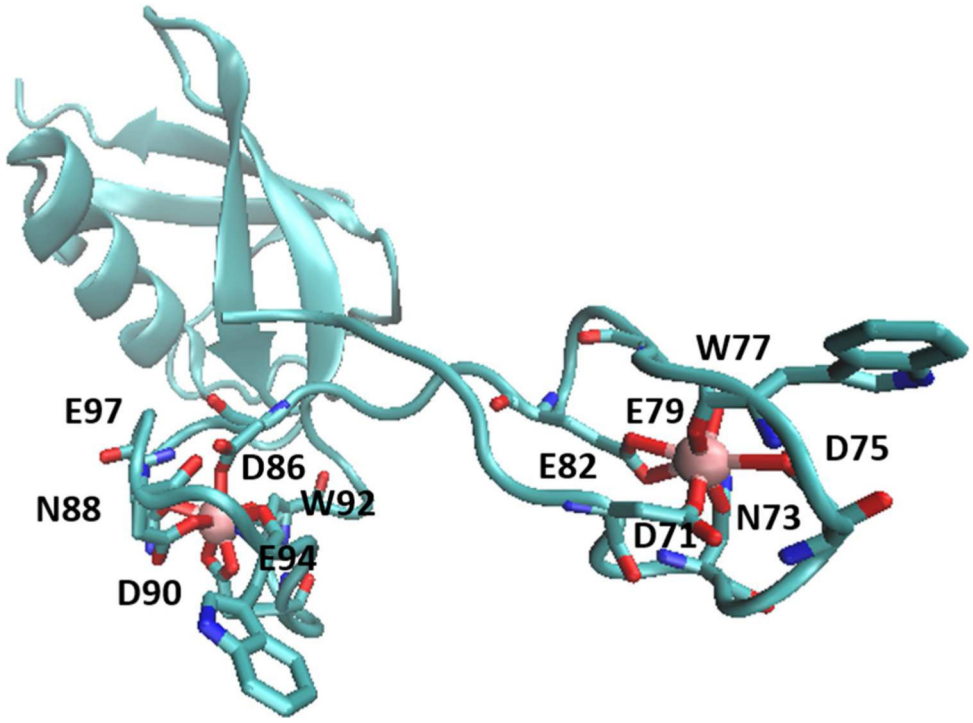

Figure 10.

Structure of a seven-coordinate lanthanide-peptide tagged to ubiquitin (PDB accession code 2OJR). Color coding: Tb^{3+} (pink spheres), N (blue), O (red), C (cyan).

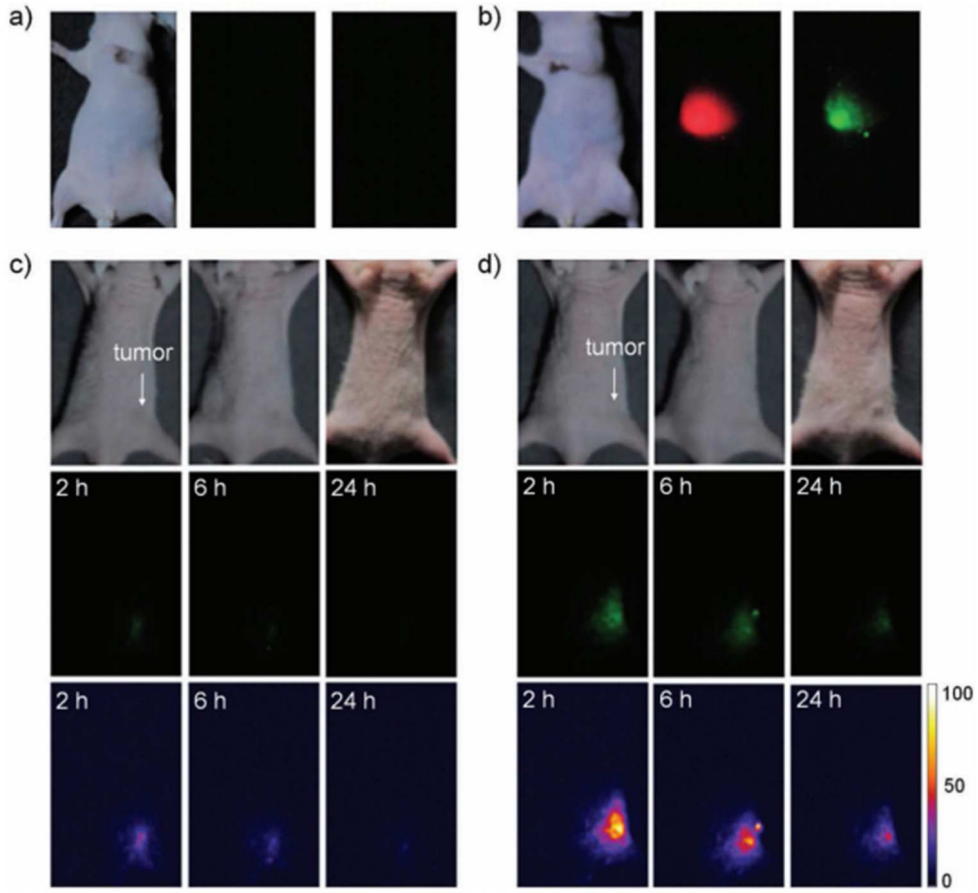

Figure 11.

a,b) Upconversion luminescence images of nude mice after 1.5 h intravenous injection a) without and b) with UCNPs. Left are bright field images, middle are red luminescence images, and right are green luminescence images. c,d) Upconversion luminescence images of nude mice bearing tumors after intravenous injection of c) UCNPs and d) UCNP-Ce6. Arrows indicate tumor sites. Top row, bright field images, middle row, true-color images of green luminescence, and bottom row, pseudo-color images converted from the corresponding true-color images (middle row) using ImageJ image analysis software (http://rsb.info.nih.gov/ij/). Red luminescence was recorded using a red band pass filter (641.5 − 708.5 nm, Semrock), and green luminescence was recorded using a combination of a green band pass filter (517 − 567 nm, Semrock) and an 850 nm short pass filter (SPF-850, CVI). Reproduced with permission from ref. 32 (© 2012 John Wiley & Sons Inc.).

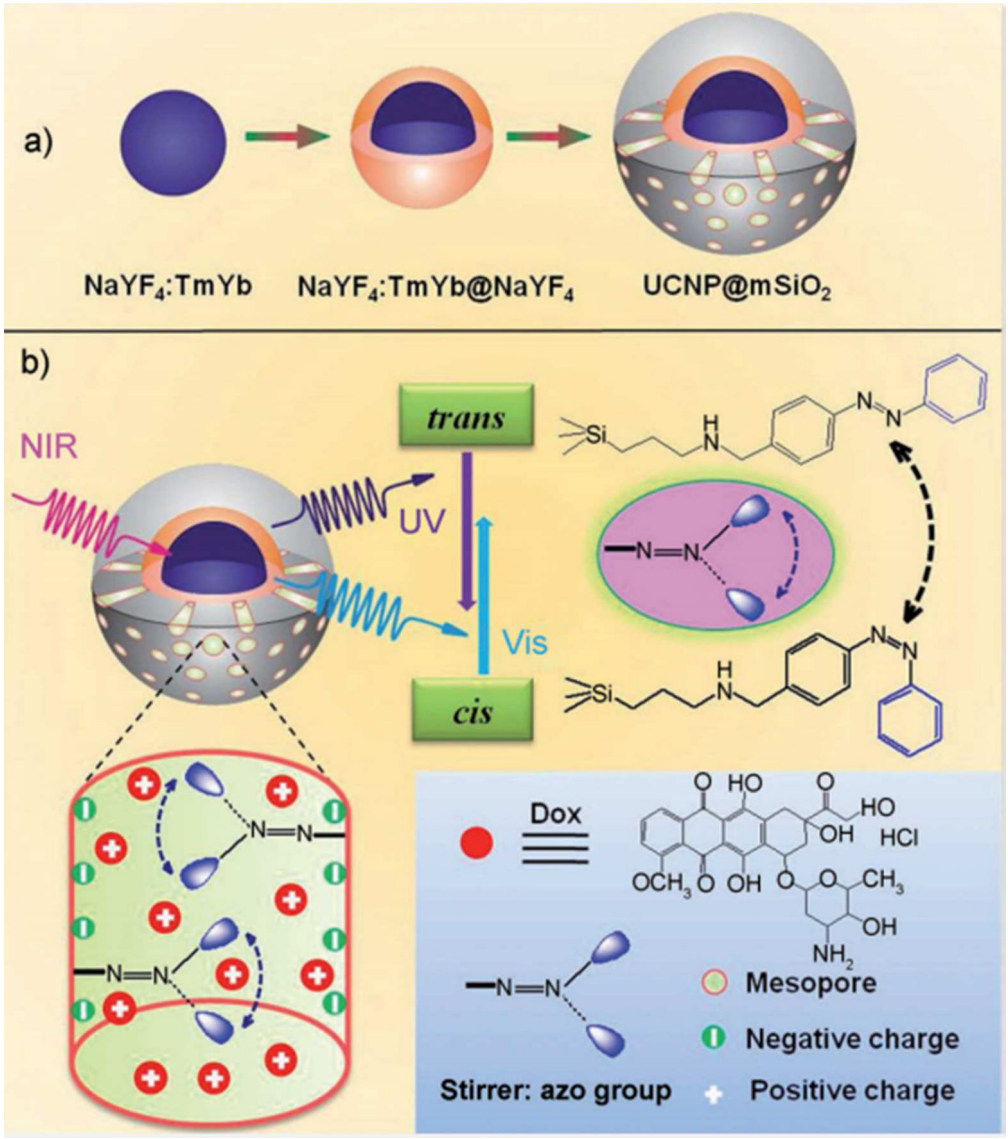

Figure 12.

a) Procedure for the synthesis of upconverting nanoparticles coated with a mesoporous silica outer layer. b) NIR light-triggered doxorubicin release by making use of the upconversion property of UCNPs and trans–cis photoisomerization of azo molecules grafted in the mesopore network of a mesoporous silica layer. Reproduced with permission from ref. 73 (© 2013 John Wiley & Sons Inc.).

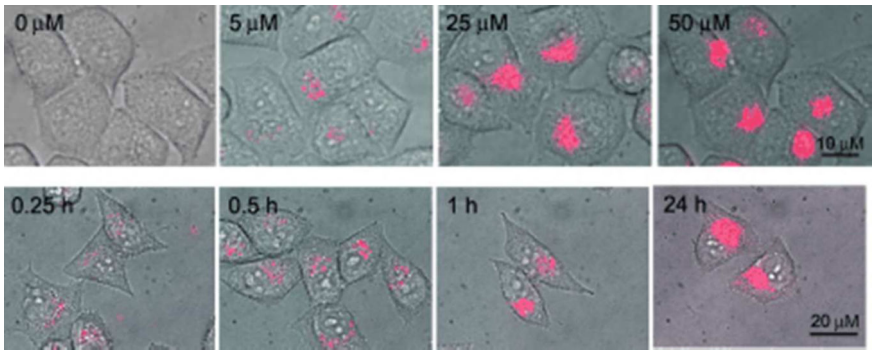

Figure 13.

Merged bright-field and time-resolved luminescence microscopy of HeLa cells loaded with $[Eu_2(L^{C5})_3]$. Top row: Cells incubated with various concentrations of $[Eu_2(L^{C5})_3]$ in RPMI-1640 for 6 h at 37 °C; conditions: Pan-Fluor lens 40× magnification, 365 nm excitation (BP 80 nm), 420 nm LP emission filter, 100 μs delay, 30 s exposure time. Bottom row: Time-course of the uptake upon incubation at 37 °C with $[Eu_2(L^{C5})_3]$ 200 μM; same conditions as above, but for magnification (100×) and excitation (340 nm, BP 70 nm). Reproduced with permission from ref. 76 (© 2009 John Wiley & Sons Inc.).